

G-Protein-Coupled Receptor Microarrays

Ye Fang, Anthony G. Frutos, and Joydeep Lahiri^{*[a]}

Membrane-bound proteins represent the single most important class of drug targets. Arraying these proteins is difficult because they typically need to be embedded in membranes to maintain their correctly folded conformations. We describe here the fabrication of microarrays consisting of G-protein-coupled receptors (GPCRs)—the single largest family of membrane-bound

proteins—by robotic pin-printing on slides, and demonstrate assays for screening of ligands on these arrays.

KEYWORDS:

drug research • G-protein-coupled receptors • high-throughput screening • membrane proteins • protein microarrays

1. Introduction

Microarray technology enables probing of the genome or proteome in a way that is naturally both systematic and comprehensive. The power and versatility of DNA microarrays is currently being realized;^[1] protein arrays^[2, 3] have, however, lagged behind in development because of issues associated with maintaining the correctly folded conformations of proteins on solid substrates. The fabrication of arrays of membrane proteins is particularly challenging because these proteins typically need to be embedded in a membrane environment in order to maintain their native conformations. Assays for screening of ligands against G-protein-coupled receptors (GPCRs), the single largest family of membrane proteins, can be classified into two major categories—whole-cell assays and homogenous assays with membrane preparations containing the receptors.^[4] Neither of these formats is well suited for simultaneously analyzing the binding of compounds to multiple receptors. There are ≈ 190 GPCRs with known natural ligands and several hundred other GPCRs for which cognate ligands remain unidentified ("orphan GPCRs").^[5] Given the large number of GPCR drug targets, many of which bind identical or analogous ligands and yet carry out distinct tissue-specific functions, the implementation of microarray methods is particularly relevant for the development of high-specificity ligands during the process of drug discovery.

2. Membrane Microarrays: General Considerations

Membrane-protein microarrays are unique in that, unlike conventional microarrays consisting of DNA or protein targets, they require immobilization of both the targets of interest and the associated lipid molecules. Confining membranes or membrane-bound proteins to microspots may be achieved in two fundamentally different ways (see Figure 1).^[6] The first method involves incubating micropatterned substrates consisting of membrane-binding and -nonbinding regions in solutions containing membranes or membrane proteins. This approach, pioneered by Groves and Boxer,^[7] is not well suited for microarray applications that require the printing of different mem-

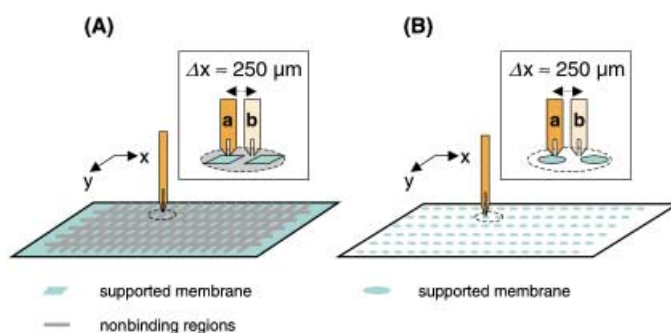


Figure 1. Schematic representation showing printing of membranes on: A) patterned substrates containing lipid binding and nonbinding regions and B) unpatterned substrates that are entirely lipid binding. Typical microarrays consist of spots that are 50–250 μm in diameter separated by 100–500 μm . The insets show the effects of a small mismatch in the registration ($\Delta x \approx 250 \mu\text{m}$) between the pin and the substrates. For patterned substrates, this small mismatch can result in deposition of the membrane onto a nonbinding area resulting in nonfabrication of the array. If the substrate is entirely membrane binding, registration is not an issue but chemistries to confine the membrane to the printed area are required.

brane compositions because it requires alignment between the printer and the lipid-binding regions. The second method is printing solutions of membranes or membrane proteins onto unpatterned membrane-binding surfaces. This approach requires that the printed lipid molecules and the embedded proteins stay confined to the printed regions. This spatial confinement may be achieved through two distinct approaches: (1) covalent^[8] or affinity-directed (for example, streptavidin–biotin, Ni–histidine^[9]) immobilization, and (2) noncovalent immobilization. Since lateral diffusion of molecules within a cell membrane is a fundamental property of real biological membranes, covalent immobilization of the entire membrane is not

[a] Dr. J. Lahiri, Dr. Y. Fang, Dr. A. G. Frutos
Biochemical Technologies
Science and Technology Division
Corning Incorporated
Corning, NY 14831 (USA)
Fax: (+1) 607-974-5957
E-mail: lahiri@corning.com

desirable for the fabrication of biomimetic supported membranes. Fortuitously, strong intermolecular interactions between lipid molecules lead to a self-limiting expansion and enable confinement of the printed membrane to the printed area. Hovis and Boxer have shown that microspots of egg phosphatidylcholine expand to only $\approx 106\%$ of the original printed area on bare-glass substrates.^[10] Although the desired lateral diffusion of lipid molecules is enabled by using this approach, a disadvantage of noncovalent immobilization (lateral spatial confinement is a more appropriate descriptor) is the poor mechanical stability of the membrane microspot. Lipids supported on solid substrates are especially susceptible to desorption when withdrawn through air–water interfaces. For example, lipids supported on bare glass spontaneously desorb when withdrawn through air–water interfaces.^[11] Typically, assays using microarrays involve incubations with different solutions and washes with different buffers; these multiple steps lead to the multiple exposures of the microarray to air. Therefore, it is important to choose surfaces such that the printed lipid microspots are mechanically stable and resist physical removal upon exposure to air.

3. Surfaces for Membrane Microarrays

The interaction of membranes with surfaces is poorly understood and involves a combination of hydrophobic, electrostatic, and surface hydration forces, the balance of which is dependent on both the surface and the composition of the membrane.^[12] Conversely, the structure of the supported membrane is strongly influenced by the nature of the surface. Surfaces that bind lipids can be broadly classified into four categories: (1) highly hydrophobic surfaces (for example, self-assembled monolayers (SAMs) of hexadecanethiolate on gold) that lead to the formation of a single lipid monolayer, (2) hydrophilic surfaces (such as bare glass) that support the adsorption of a single lipid bilayer, (3) hybrid surfaces presenting amphiphilic anchor molecules^[13] that bind a lipid bilayer offset from the surface at a distance determined by the length of the hydrophilic moiety (of the anchor molecules), and (4) surfaces presenting “polymer cushions” that create a supported lipid bilayer offset from the hard substrate by a polymeric matrix. Idealized representations of supported lipids on these types of surfaces are shown in Figure 2. The primary practical consideration, beyond lateral fluidity and mechanical stability, is the ability of the printed membranes to incorporate integral membrane proteins in their correctly folded conformations. Supported monolayers are of limited utility because they cannot incorporate membrane-spanning proteins. Membranes formed on hydrophilic surfaces (for example, bare glass) can incorporate only those proteins with extramembrane domains less thick than the layer of adsorbed water (≈ 10 Å). Surfaces that are mobile and penetrable, that is, surfaces that can be deformed such as those presenting flexible amphiphilic tethers or polymer cushions can potentially be used for immobilization of a broad range of membrane proteins.^[12]

Our choice of surfaces for membrane-protein microarrays was based on an initial investigation of properties of model membranes on surfaces. We were interested in surfaces on

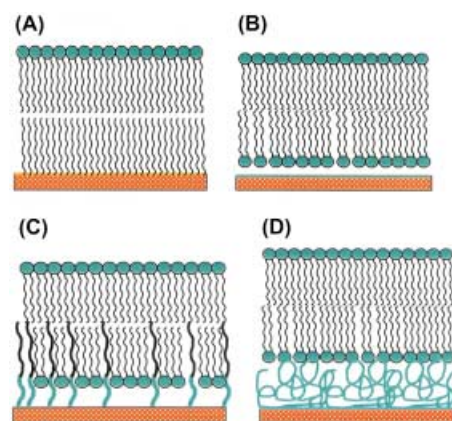


Figure 2. Idealized representations of supported membranes on different types of surfaces. The figures show: A) highly hydrophobic surfaces consisting of close-packed hydrocarbon tails that result in lipid monolayers, B) hydrophilic surfaces, such as bare glass, that result in lipid bilayers offset by ≈ 10 Å due to adsorbed water, C) surfaces presenting amphiphilic tethers that result in lipid bilayers offset by the hydrophilic moieties of the tether molecules, and D) surfaces presenting a polymer cushion that result in a lipid bilayer adsorbed on a spongy matrix.

which the model membranes exhibited lateral fluidity and high mechanical stability. Among those tested, surfaces modified with γ -aminopropylsilane (GAPS) provided the desired combination of properties of the supported lipids.^[14] Experiments based on fluorescence recovery after photobleaching revealed significant lateral fluidity (with a mobile fraction of $\approx 50\%$), and experiments in which the printed membrane arrays were withdrawn multiple times through air–water interfaces without desorption demonstrated high mechanical stability. Significantly, this high stability was observed for both gel- and fluid-phase lipids. It should be noted that the nature of the GAPS surface and methods of derivatization are important in determining the properties of the model membranes and the bioassays described below. The methods we used for modifying surfaces with GAPS are proprietary to Corning and cannot be currently disclosed.

4. GPCR Microarrays: Fabrication and Assays

4.1. Array fabrication

Due to their pharmacological relevance, diversity, and complexity, the fabrication of GPCR microarrays represents a significant feasibility test for membrane-protein microarrays. We obtained GPCRs as membrane-associated suspensions in buffer from commercial vendors (Biosignal Packard or Perkin Elmer Life Sciences). The cell line used for overexpression of the receptor, the concentration of the active receptor (B_{\max}), and the total concentration of the protein in the preparation were provided by the vendor. Multiple arrays of GPCRs were printed on coated slides by using a quill-pin printer. After printing, the arrays were incubated in a humid chamber at room temperature for one hour, and subsequently used for ligand-binding experiments. Typically, each array was incubated for one hour with $10\ \mu\text{L}$ of a buffered solution containing fluorescently labeled ligands or mixtures of fluorescently labeled ligands and unlabeled inhibitors for competitive binding assays. After incubation, the

solutions were carefully removed with a pipette tip attached to a vacuum pump. The slides were rinsed briefly with water, dried under a stream of nitrogen, and imaged in a fluorescence scanner.

4.2. Dose dependency and relative potency

Figure 3 shows data from the binding of bodipy tetramethylrhodamine labeled neurotensin (BT-NT) to microarrays of the human neurotensin receptor, subtype 1. The amount of binding is dependent on the concentration of the ligand used. In order to estimate the binding constant for BT-NT, we determined the amount of specific binding by subtracting the fluorescence signals from a second set of arrays incubated with BT-NT at the same concentrations in the presence of excess unlabeled neurotensin. From a Scatchard analysis of the subtracted data, we estimate the dissociation constant K_d to be ≈ 1.3 nM, which is a similar value to that obtained by using other techniques such as fluorescence polarization.

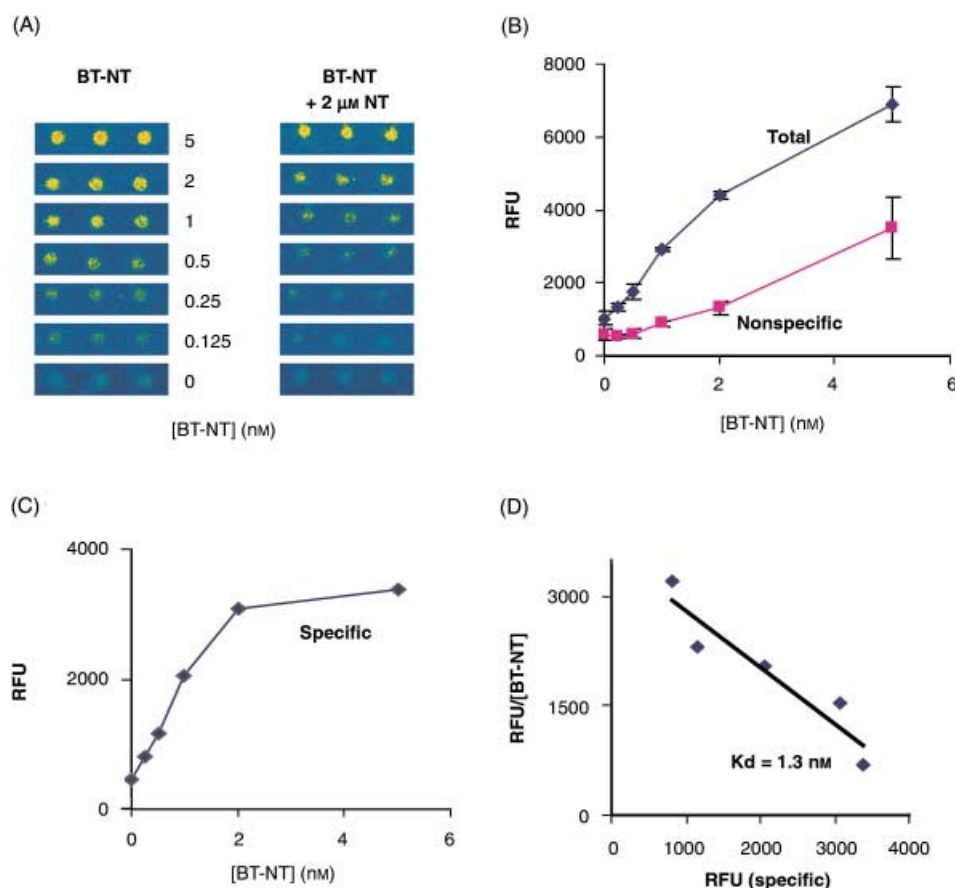


Figure 3. Saturation profile for the binding of fluorescently labeled neurotensin (bodipy tetramethylrhodamine neurotensin, BT-NT) to arrays of the neurotensin receptor (human subtype I, NTR1). A) Fluorescence images of 14 arrays consisting of NTR1 microspots printed in triplicate on a single GAPS-coated slide after incubation with solutions containing BT-NT at different concentrations in the absence (left panel) and presence (right panel) of unlabeled neurotensin (2 μ M NT). B) Plot of the fluorescence intensity of NTR1 arrays as a function of the concentration of BT-NT in the absence (equal to the total signal) and presence (representing the nonspecific signal) of excess unlabeled NT. C) Plot of the fluorescence intensity of the NTR1 arrays due to the specific binding as a function of BT-NT. D) Scatchard plot for estimation of the binding constant for BT-NT.

Figure 4 shows the inhibition of binding of BT-NT by neurotensin and neuromedin N; from the data, we estimate that the IC_{50} values are ≈ 2.5 nM and 25 nM for neurotensin and neuromedin N, respectively, consistent with the literature.^[15]

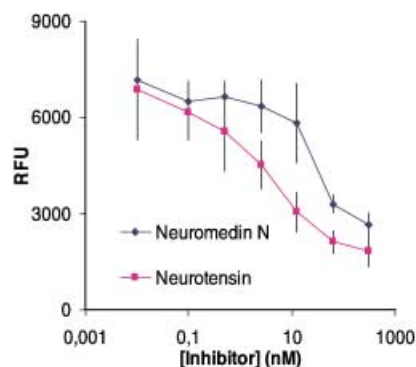


Figure 4. Graph showing the concentration-dependent inhibition of binding of BT-NT by neurotensin and neuromedin N to microarrays of the neurotensin receptor (NTR1). The relative differences in affinity are consistent with the known relative potencies of these inhibitors.

The ability to obtain binding constants consistent with previous reports is significant for several reasons. First, there are few reports describing the use of microarrays for obtaining binding constants for *any* protein array; although the universality of obtaining binding constants for compounds by using GPCR microarrays needs to be determined, our data certainly demonstrate the feasibility of obtaining semiquantitative information about ligand binding. Second, the affinity of a ligand for a GPCR depends on whether the receptor is complexed to G proteins;^[4, 16] therefore, the agreement between the binding constants obtained with GPCR microarrays and homogeneous assays suggests that the fraction of free and complexed GPCRs remain essentially unchanged upon printing.

4.3. Receptor selectivity screening

Protein microarrays naturally offer the simultaneous detection of binding to multiple proteins and are therefore well suited for determining the selectivity of a compound among the different sub-

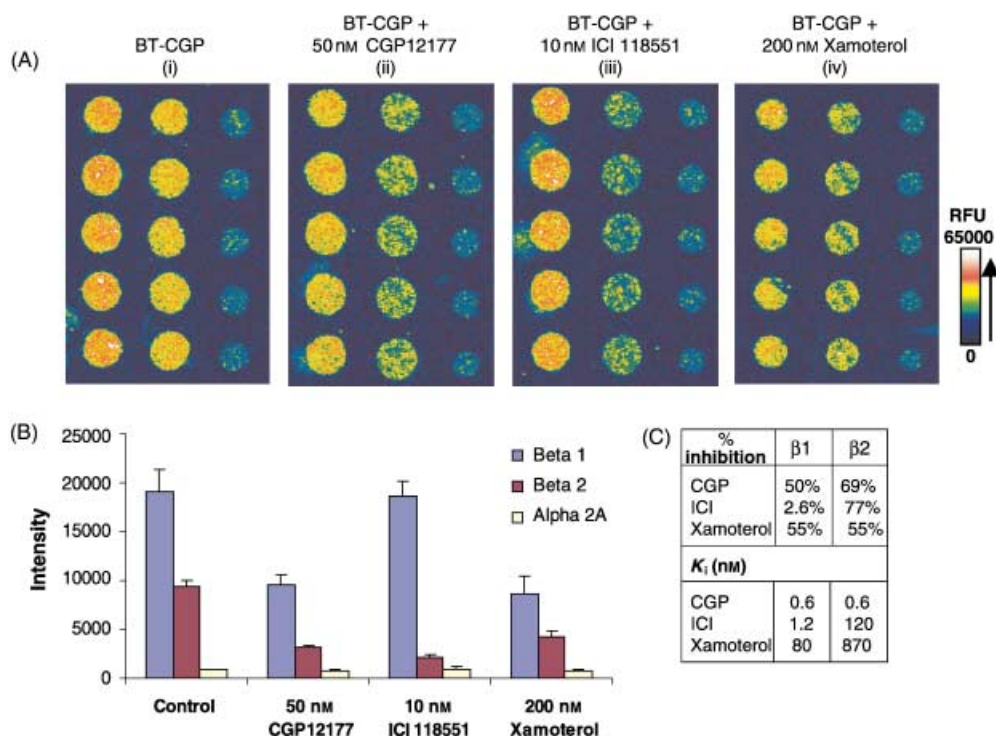


Figure 5. Demonstration of the use of GPCR microarrays for determining the selectivity of compounds among the different subtypes of a receptor. Each microarray consists of three columns; each column contains, from left to right, five replicate microspots of the $\beta 1$, $\beta 2$, and $\alpha 2A$ adrenergic receptors, respectively. A) Fluorescence false-color images (from left to right) of the array incubated with solutions containing BT-CGP (5 nM) and mixtures of BT-CGP (5 nM) with CGP 12177 (50 nM), ICI 118551 (10 nM), and xamoterol (200 nM) to the array. B) Histogram analysis of the images in (A) showing the relative fluorescence intensities (RFU) of the arrays incubated with BT-CGP or mixtures of BT-CGP and inhibitors. C) Table showing the amounts of inhibition and the K_i values for the inhibitors used in the experiment.

types of a receptor family. Figure 5 shows the binding of different ligands to arrays of the adrenergic receptor—from left to right within an array, each column of microspots corresponds to the $\beta 1$, $\beta 2$, and $\alpha 2A$ subtypes, respectively. When the array was incubated with a solution of bodipy tetramethylrhodamine labeled CGP 12177 (BT-CGP), a known β -selective antagonist,^[17] only spots corresponding to the β subtypes exhibited fluorescence, as seen in Figure 5 A (i). Figures 5 A (ii–iv) show images of arrays treated with solutions containing BT-CGP (5 nM) and either CGP 12177 (50 nM), ICI 118551 (10 nM), or xamoterol (200 nM), respectively. The affinities of these compounds for the adrenergic receptor have been reported previously and are tabulated in Figure 5 C. Although a typical screening assay comparing different compounds would be conducted at the same concentration, we chose to work with concentrations of these compounds that demonstrate their known differential selectivities for the different receptors. Since CGP 12177 is a nonselective β -antagonist (inhibition constant $K_i \approx 0.6$ nM), we estimate that the amount of inhibition at 50 nM CGP 12177 represents the fraction of “active” receptors that are capable of ligand binding. The higher affinity of ICI 118551 for the $\beta 2$ receptor ($K_i \approx 1.2$ nM)^[18] relative to the $\beta 1$ receptor ($K_i \approx 120$ nM) is clearly demonstrated upon comparing the inhibition data to that obtained for CGP 12177. The inhibition of binding by xamoterol is also consistent with its affinities for the $\beta 1$ and $\beta 2$ receptors. Taken together, these data demonstrate the feasibility of using GPCR microarrays for determining the specificities of compounds within the subtypes of a given receptor.

5. Conclusion

The greatly increased pace of target identification and the demand for high-specificity drugs will necessitate the development of upstream selectivity studies with protein arrays. For GPCRs, the paradigm of “classical pharmacology” is relevant only for already classified receptors; for orphan receptors, a strategy based on “reverse pharmacology” may be more relevant or powerful.^[5] GPCR microarray assays, which offer the possibility of multiplexing of both receptors and compounds, may be used to combine aspects of both strategies. The use of GPCR microarrays containing orphan and already classified receptors against multiple compounds may greatly streamline the process of classifying both receptors and compounds. We have demonstrated the use of GPCR microarrays for compound binding; a current limitation of this technology is the inability to classify the activities of compounds as agonists or antagonists. Nevertheless, the inference that the printed GPCRs remain complexed with their G proteins^[14] suggests an exciting possibility—the use of GPCR microarrays for studying not just binding but also biological function.

- [1] C. Deboucq, P. Goodfellow, *Nat. Genet.* **1999**, 21, 48–50.
- [2] G. MacBeath, S. L. Schreiber, *Science* **2000**, 289, 1760–1761.
- [3] H. Zhu, M. Bilgin, R. Bangham, D. Hall, A. Casamayor, P. Bertone, N. Lan, R. Jansen, S. Bidlingmaier, T. Houfek, T. Mitchell, P. Miller, R. A. Dean, M. Gerstein, M. Snyder, *Science* **2001**, 293, 2101–2105.
- [4] *G-Protein-Coupled Receptors* (Eds.: T. Haga, G. Berstein), CRC Press, Boca Raton, FL, **1999**.

- [5] A. D. Howard, G. McAllister, S. D. Feighner, Q. Liu, R. P. Nargund, L. H. Van der Ploeg, A. A. Patchett, *Trends Pharmacol. Sci.* **2001**, *22*, 132–140.
- [6] J. Lahiri, S. J. Jonas, A. G. Frutos, P. Kalal, Y. Fang, *Biomed. Microdevices* **2001**, *3*, 157–164.
- [7] J. T. Groves, S. G. Boxer, *Acc. Chem. Res.* **2002**, *35*, 149–157.
- [8] L. Holger, C. Duschl, H. Vogel, *Langmuir* **1994**, *10*, 197–210.
- [9] T. Stora, Z. Dienes, H. Vogel, C. Duschl, *Langmuir* **2000**, *16*, 5471–5478.
- [10] J. Hovis, S. G. Boxer, *Langmuir* **2000**, *16*, 894–897.
- [11] P. S. Cremer, S. G. Boxer, *J. Phys. Chem. B* **1999**, *103*, 2554–2559.
- [12] J. Y. Wong, C. K. Park, M. Seitz, J. Israelachvili, *Biophys. J.* **1999**, *77*, 1458–1468.
- [13] J. Lahiri, P. Kalal, A. G. Frutos, S. J. Jonas, R. Schaeffler, *Langmuir* **2000**, *16*, 7805–7810.
- [14] Y. Fang, A. G. Frutos, J. Lahiri, *J. Am. Chem. Soc.* **2002**, *124*, 2394–2395.
- [15] S. Barroso, F. Richard, D. Nicolas-Etheve, J. L. Reversat, J. M. Bernassau, P. Kitabgi, C. Labbe-Jullie, *J. Biol. Chem.* **2000**, *275*, 328–336.
- [16] S. P. Fay, R. G. Posner, W. N. Swann, L. A. Sklar, *Biochemistry* **1991**, *30*, 5066–5075.
- [17] M. Staehelin, K. Jaeggi, N. Wigger, *J. Biol. Chem.* **1983**, *258*, 3496–3502.
- [18] A. Bilski, S. Dorries, J. D. Fitzgerald, R. Jessup, H. Tucker, J. Wale, *Br. J. Pharmacol.* **1980**, *69*, 292.

Received: May 13, 2002 [C 417]